Electronic Supplementary Information

Machine Learning Analysis and Prediction Models of Alkaline Anion Exchange Membranes for Fuel Cells

*Xiuyang Zou, Ji Pan, Zhe Sun, Bowen Wang, Zhiyu Jin, Guodong Xu and Feng Yan **

College of Chemistry, Chemical Engineering and Materials Science, Soochow University, Suzhou, 215123, China

* ***E-mail:*** fyan@suda.edu.cn

1 Experimental Section

1.1 Materials

Poly (2,6-dimethyl-1,4-phenylene oxide) (PPO) (Mn=20,000) was supplied by J&K Scientific Ltd. N-Bromosuccinimide (NBS), benzoyl peroxide, 2, 2'-azobis-isobutyronitrile (AIBN), trimethylamine (TMA, 7.3 M aqueous solution), Triethylamine (TEA), chlorobenzene, diethyl ether, N-methyl-2-pyrrolidone (NMP, reagent grade) were acquired from Sigma-Aldrich Chemical Reagent Co., Ltd.

1.2 Synthesis of AEMs

An amount of 5.04 g of PPO was dissolved in 140 mL of chlorobenzene. Then 0.51 g (2.11 mmol) of benzoyl peroxide (BPO) and 2.93 g (16.42 mmol) of NBS were added under vigorous stirring at 85 ℃. After reacting for 24 h, the yellow solid (Br-PPO) was collected by filtration, washed thrice with methanol, and dried at 50 ℃ for 48 h.

0.25 g Br-PPO was dissolved in 10 mL NMP and reacts with excess TMA (or excess triethylamine) at room temperature for 4 days: The molar ratio of TMA (or triethylamine) to polymer is 2: 1. The reacted

mixture was added drop-wise to diethyl ether and the quaternized PPO were obtained by filtering and washing via diethylether. An amount of 0.15 g of quaternized PPO copolymers was dissolved in 10 mL NMP and dried in an oven at 80 ℃ for 36 hours, and then the resulting membrane was soaked in 1 M NaOH at room temperature for 48 hours.

1.3 Characterization and Measurements

All polymers were characterized by 1H-NMR spectroscopy with a Bruker DR X400 spectrometer at room temperature using $CDCl_3$ or DMSO-d_6 as solvents.

Under a nitrogen atmosphere, the membrane was dried for 48 hours and weighed to obtain the mass (m_{dry}) of the dried sample. Then, the membrane was soaked in deionized water for 48 hours under nitrogen, and weighed to obtain the mass (m_{wet}) of the wet sample. The water uptake (*WU*, %) was calculated by the following formula:

$$WU = \frac{m_{wet} - m_{dry}}{m_{dry}} * 100 \qquad (1)$$

Similarly, the swell ratio (*SR*) was calculated by the following formula:

$$SR = \frac{L_{wet} - L_{dry}}{L_{dry}} * 100 \qquad (2)$$

Where L_{wet} and L_{dry} are the lengths of the wet and dry sample at room temperature, respectively.

The small membrane sample was soaked in 1 M NaOH solution at 60 ℃ for a specified time from 24 h to 168 h. After treatment, it was carefully washed with deionized water under nitrogen. When the pH of the membrane reached 7, it was soaked in deionized water for 40 minutes, and its ion conductivity was measured. The resistance value (*R*) of the membrane was measured by using electrochemical workstation (Shanghai Chen hua) via the four-electrode method. The ion conductivity was calculated by the formula (3):

$$\sigma = \frac{d}{LWR} \qquad (3)$$

Where *d* is the distance between reference electrodes, and *L* and *W* are the thickness and width of the membrane, respectively.

1.4 ANN model

The detailed introduction of the ANN model is as follows: First, all input features are normalized to form a 15-dimensional vector $\mathbf{X_i}$. As illustrated in **Figure 1b**, the number of neurons in the input layer is equal to the number of input features. When a set of input features are input to the input layer, each neuron in hidden layer 1 calculates an independent result through its activation function $f(W\mathbf{X_i}+\mathbf{b})$. The type of activation function determines a neuron's reaction to the complete incoming signal. The commonly used activation functions are as follows:

Relu activation function (The Rectified Linear Unit): $f(x) = \max(0, x)$

Tanh activation function: $f(x) = \frac{e^{x} - e^{-x}}{e^{x} + e^{-x}}$

Sigmoid activation function: $f(x) = \frac{1}{1 + e^{-x}}$

Softsign activation function: $f(x) = \frac{x}{1 + |x|}$

Softplus activation function: $f(x) = \log(1 + e^{x})$

Then the 70 calculation results of hidden layer 1 are merged into a 70-dimensional vector as the new input of hidden layer 2. The same procedure was repeated until the dataflow reached the output layer. The number of neurons in the output layer is equal to the number of output features. By considering the prediction error of the results of each hidden layer, the previous neurons are retrained and their parameters are updated.

Here previous neurons were calculated by formula:

$$\delta_i^{(nl)} = \frac{\partial}{\partial z^{(nl)}} \frac{1}{2} \left\| y - h_{W,b}(x) \right\|^2 = -\left(y_i - \alpha_i^{(nl)} \cdot f'(Z_i^{(nl)}) \right)$$

where $f(z) = f(W^T x) = h_{W,b}(x)$, *W* is weight, *b* is bias (parameters in neuron).

2 Supplementary figures and tables

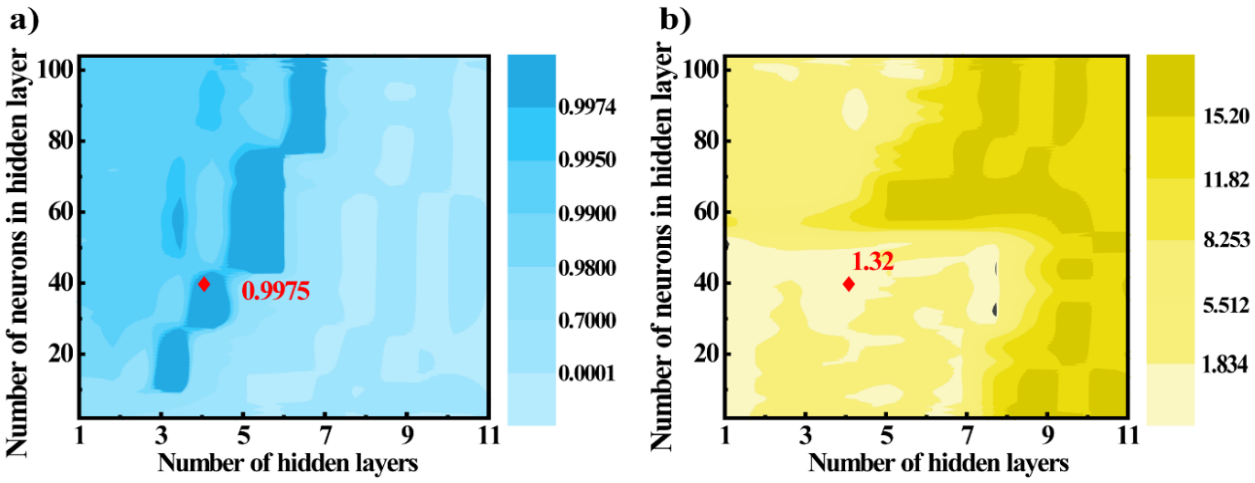

Figure S1. Distribution of (a) R^2 values and (b) *Rmse* of the ANN for variable numbers of hidden layers and neurons in the hidden layer. The best ANN model (maximum R^2 and minimum *Rmse*) were obtained by grid search of combinations of different numbers of hidden layers and neurons.

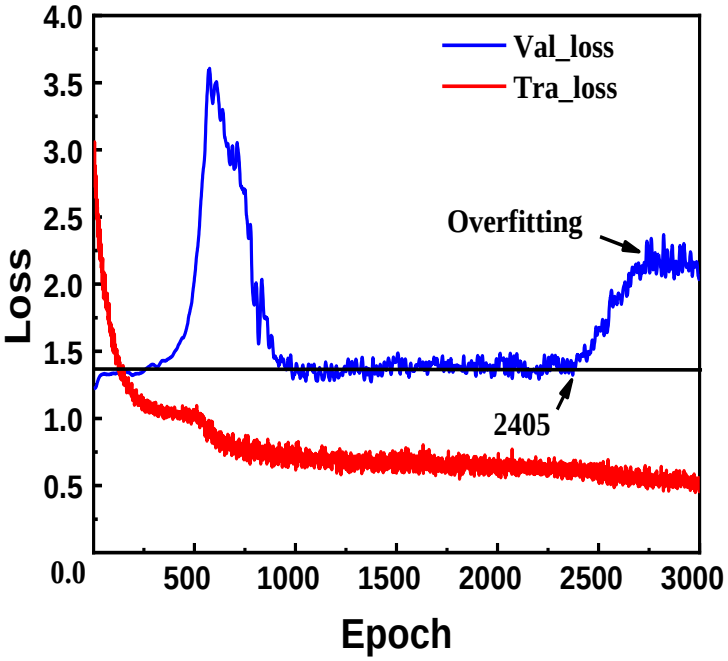

Figure S2. The loss curves on the training set and the split training set used for validation in the training process of the artificial neural network

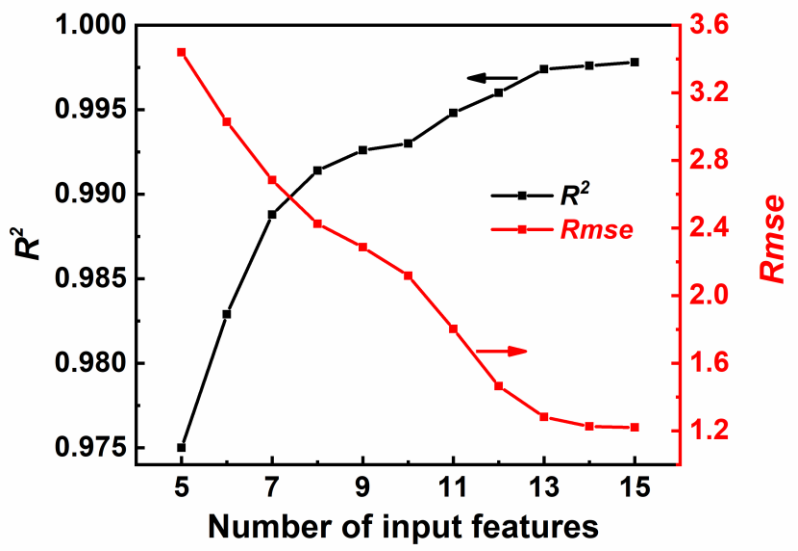

Figure S3. Summary of the *Rmse* and R^2 values for ANN model with different number of input features.

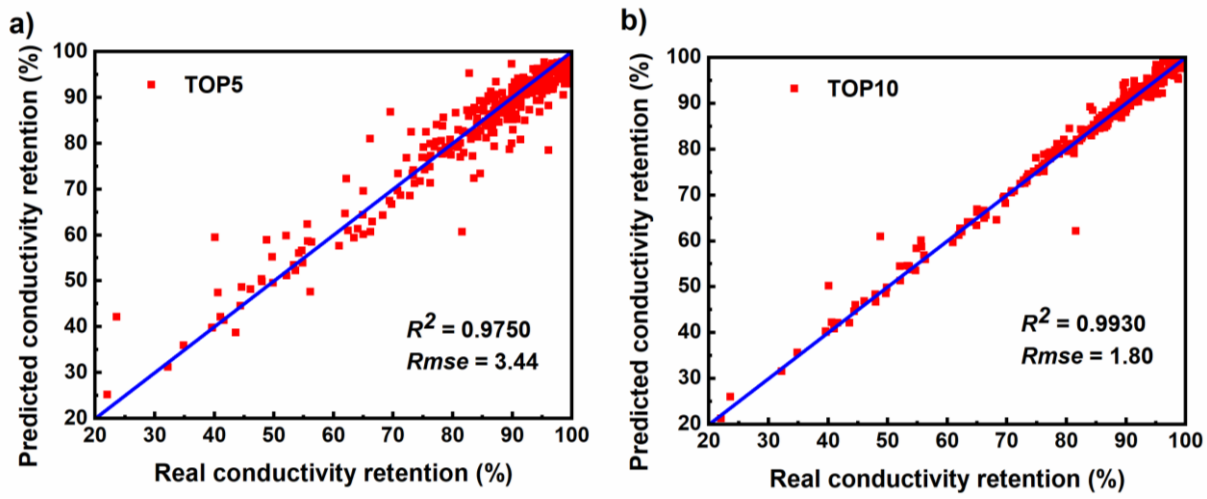

Figure S4. Regression correlation coefficient (R^2) of (a) TOP5, (b) TOP10 for test set under the same structure of the database. The top 5 features (TOP5) or the top 10 features (TOP10) are used as inputs to build regression models, respectively. The R^2 value of the model increases with the number of input features. In order to increase the accuracy of the model, a more complex model (15 input features) was selected.

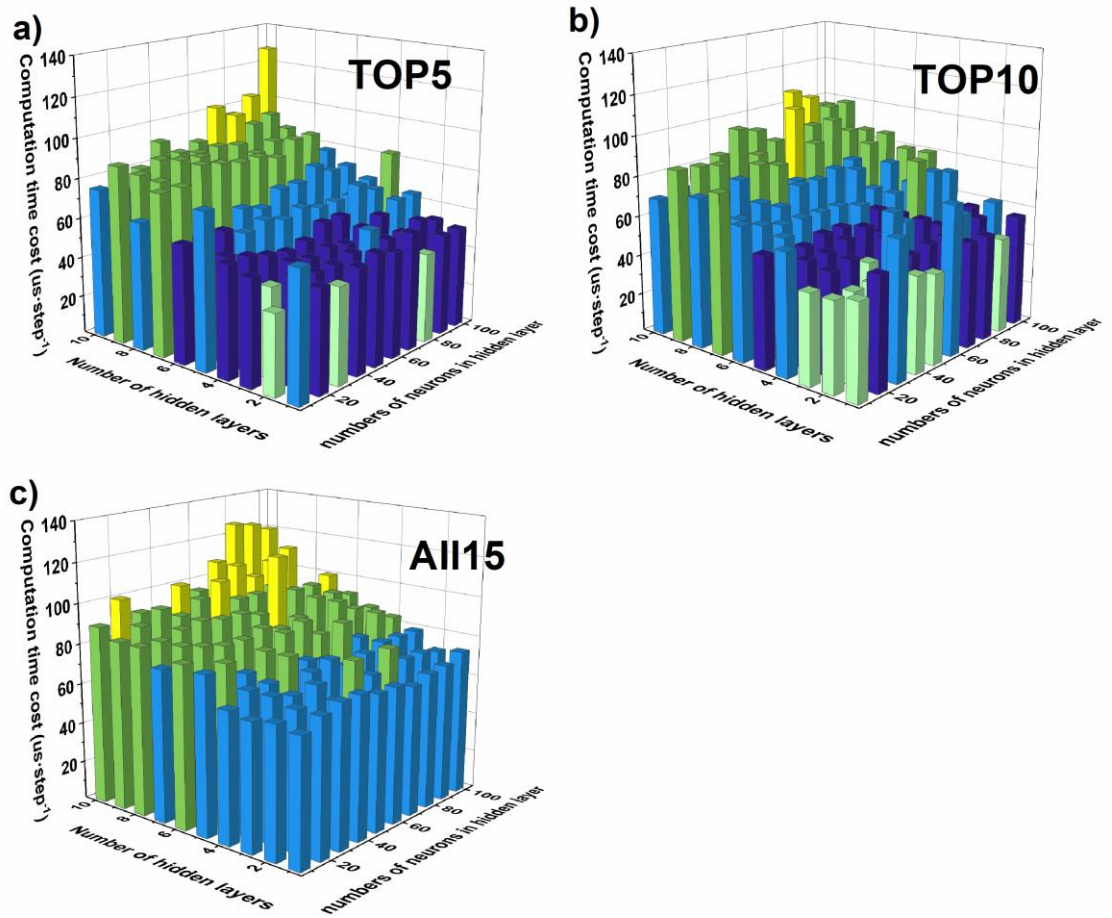

Figure S5. Computation cost under different combinations of the numbers of neurons and hidden layers by a) TOP5, and b) TOP10 (a server equipped with GTX 1050Ti and the CUDA7.5 framework). It can be observed that the differences between the times under different combinations of the numbers of neurons and hidden layers were small (in the same order of magnitude). Considering the accuracy of the model, it is worth for sacrificing some time cost.

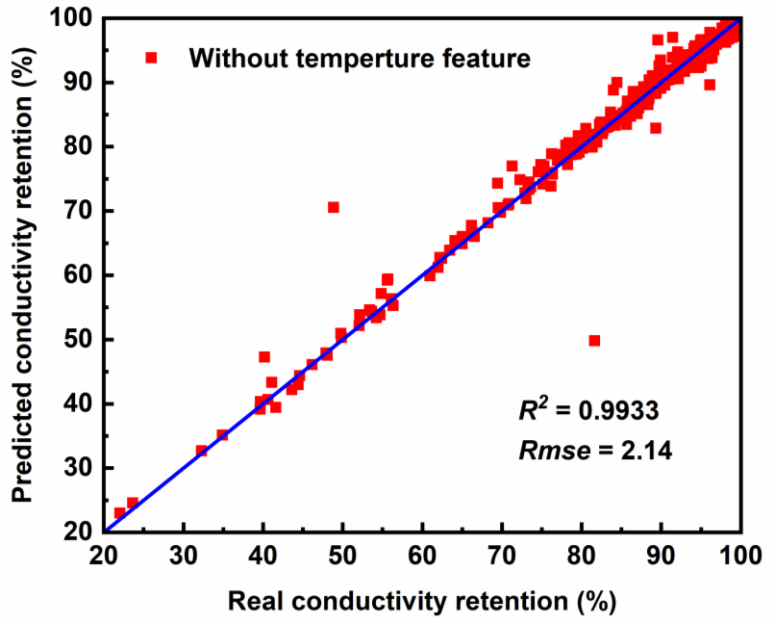

Figure S6. Regression correlation coefficient (R^2) of without temperature feature for test set under the same structure of the database in Figure 4.

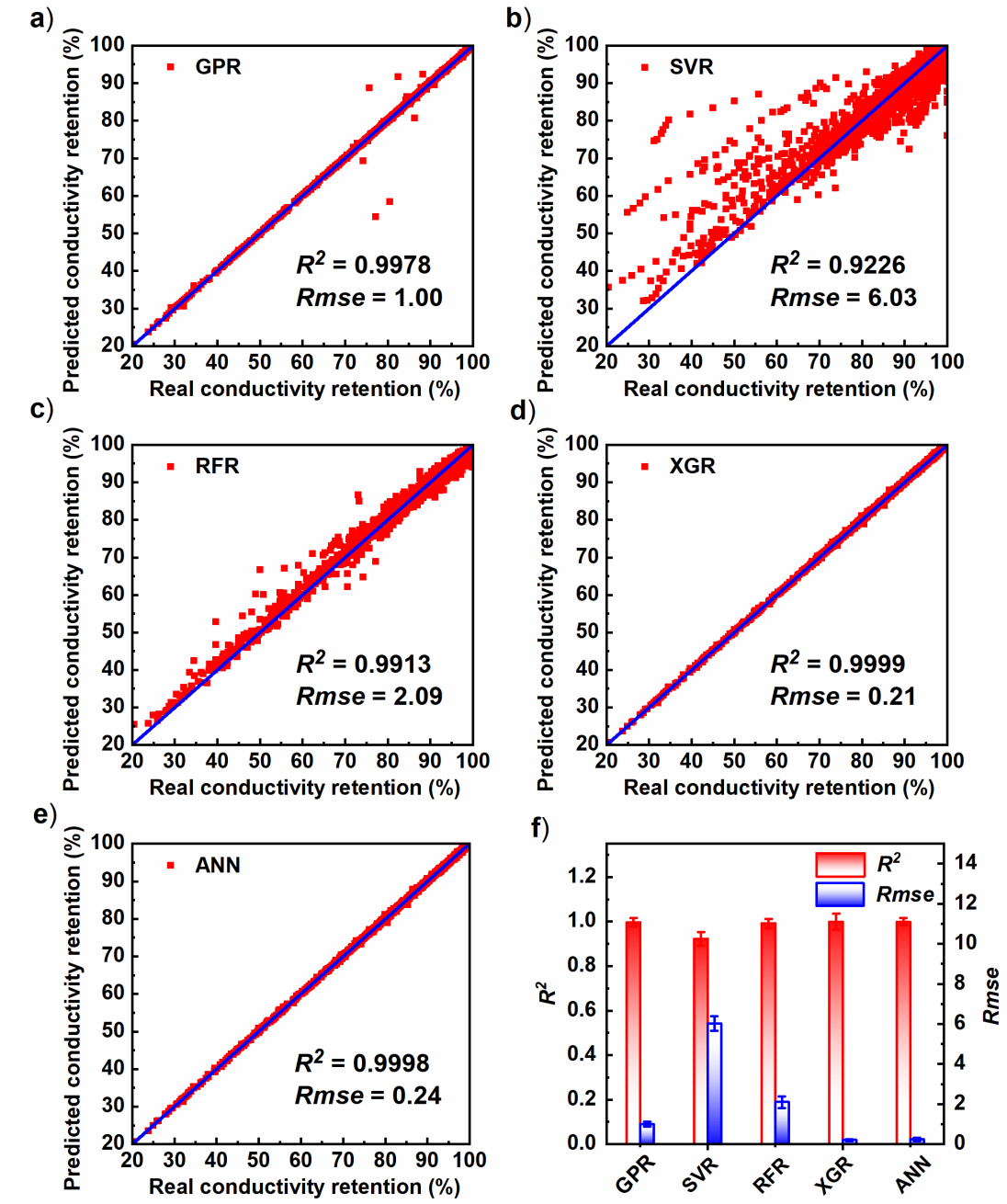

Figure S7. Regression correlation coefficient (R^2) of (a) GPR, (b) SVR, (c) RFR, (d) XGR, and (e) ANN algorithms for training set under the same structure of the database. (f) Summary of the *Rmse* and R^2 values for each machine learning algorithm. By modifying the random seed number, different training and test sets were generated to verify the robustness of the algorithms.

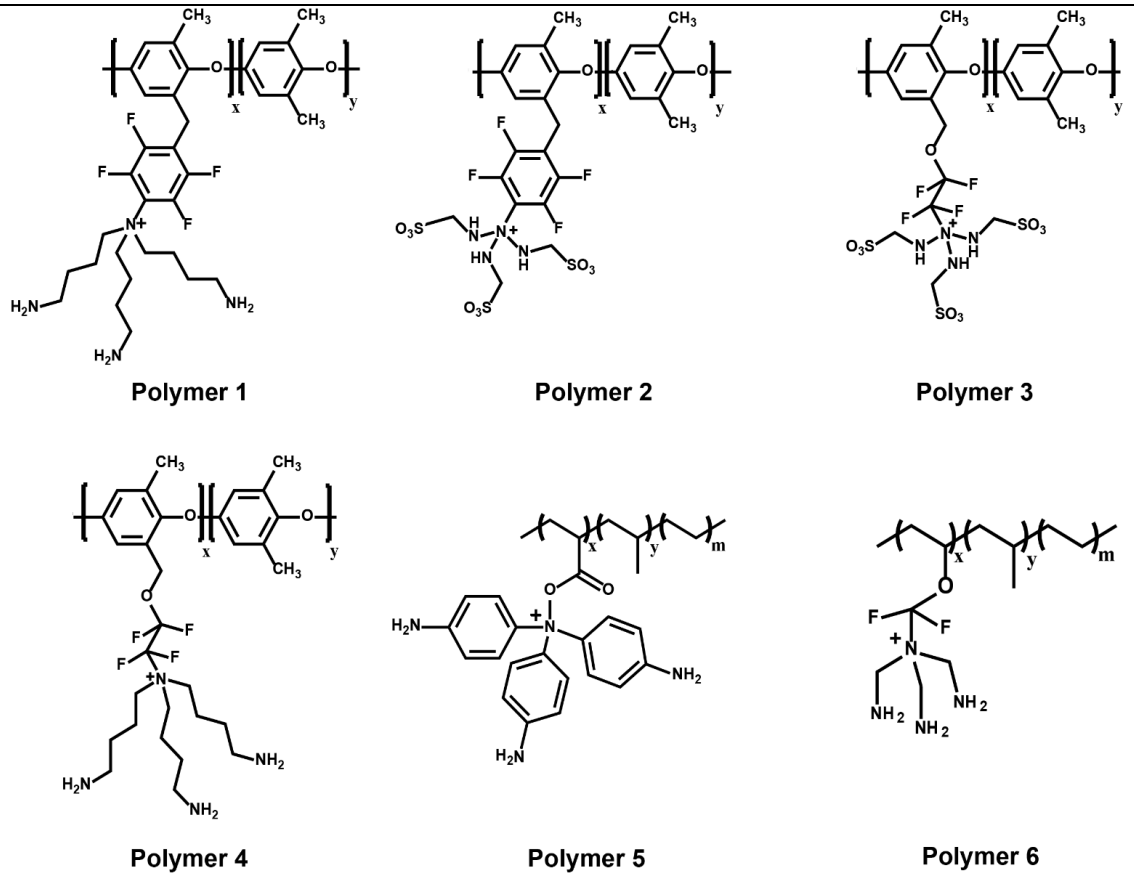

Figure S8. The chemical structure of the polymers predicted by the artificial neural network (listed in Table S5). However, there are 15 input parameters for the ANN model, these parameters may be contradictory to each other. For example, the swelling ratio and water uptake of **Polymer 1** is set to be 1.92% and 55.64%, respectively. However, such a design is difficult to be realized experimentally. Due to the inherent shortcomings of the ANN model, the optimal chemical structures of AEMs given by the AI were not adopted in this work. Although ANN was not used to obtain the possible best performances, it can still guide our experimental design, due to its high accuracy (R^2 =0.9978).

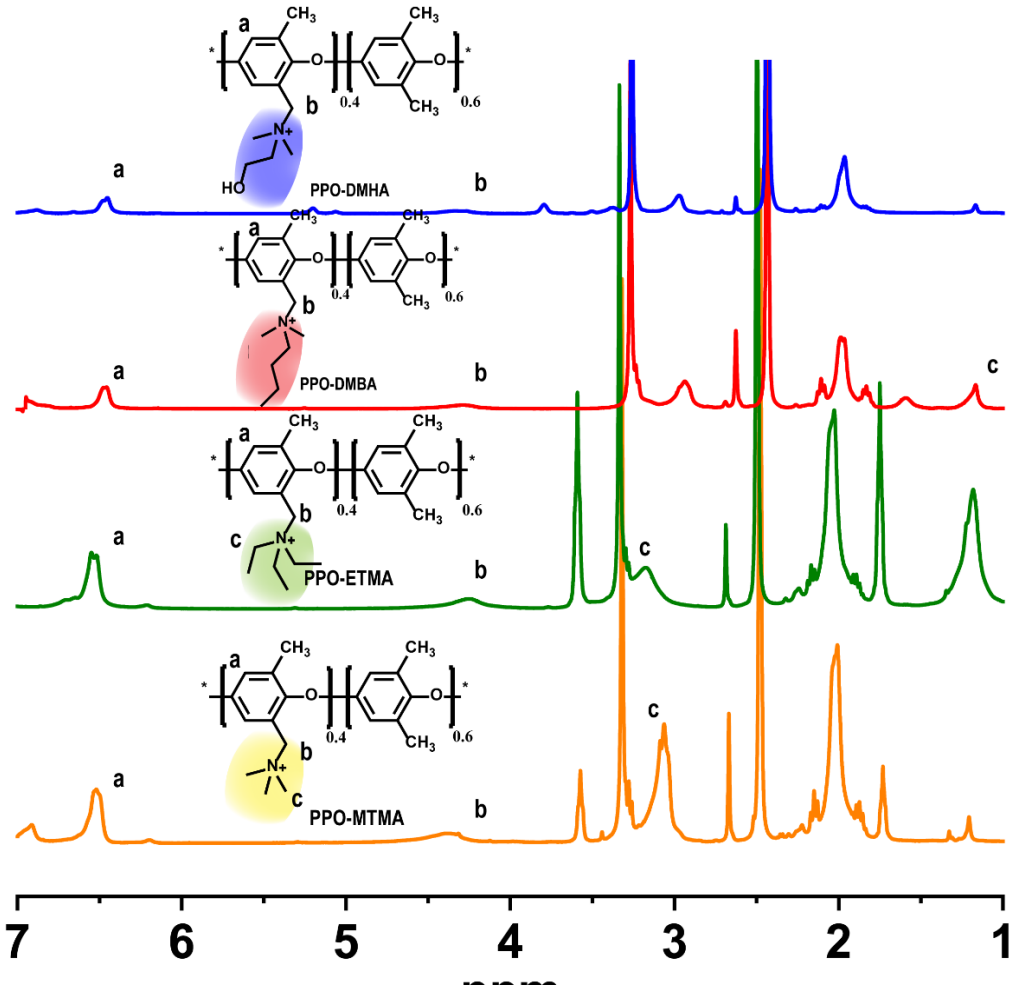

Figure S9. The chemical structures and NMR spectra of four AEMs investigated in this work.

Table S1. Hammett and modified Swain-Lupton constants of substitution group*

	σ_m	σ_p	F	R	ref(s)
Br	0.39	0.23	0.45	-0.22	[1]
CF_3	0.43	0.54	0.38	0.16	[1]
CF_2CF_3	0.47	0.52	0.44	0.08	[2]
$CF_2CF_2CF_3$	0.44	0.48	0.42	0.06	[1]
CH_2NH_2	-0.03	-0.11	0.04	-0.16	[1]
CH_3	-0.07	-0.17	0.01	-0.18	[1]
C_2H_5	-0.07	-0.15	0	-0.15	[1]
C_3H_7	-0.06	-0.13	0.01	-0.14	[1,3]
$(CH_2)_3CH_3$	-0.08	-0.16	-0.01	-0.15	[3,4]
$(CH_2)_4$	-0.48	-0.48	-0.4	-0.08	[3]
$SO_2C_6H_5$	0.62	0.68	0.58	0.1	[1]
OC_6H_5	0.25	-0.03	0.37	-0.4	[1,3]
CN	0.56	0.66	0.51	0.15	[1]
C_6H_5	0.06	-0.01	0.12	-0.13	[1]
C_6F_5	0.26	0.27	0.27	0	[4]
C_6H_4-4-Br	0.15	0.12	0.18	-0.06	[1]
C_6H_4-4-Cl	0.15	0.12	0.18	-0.06	[1]
C_6H_4-4-F	0.12	0.06	0.17	-0.11	[1]
$OCH_2CH_2CH_3$	0.1	-0.25	0.26	-0.51	[1]
$CONH_2$	0.28	0.36	0.26	0.1	[3,5]
COC_6H_5	0.28	0.3	0.31	-0.01	[1]
NO	0.62	0.91	0.49	0.42	[5]
SO_3^-	0.3	0.35	0.29	0.06	[1]
SO_2^-	-0.02	-0.05	0.03	-0.08	[2]
Cl	0.37	0.23	0.42	-0.19	[1]

$NHNH_2$	-0.02	-0.55	0.22	-0.77	3
CO_2^-	-0.1	0	-0.1	0.1	1
NH_2	-0.16	-0.66	0.08	-0.74	1
$CHBr_2$	0.31	0.32	0.31	0.01	3
$CHCl_2$	0.31	0.32	0.31	0.01	3
CHF_2	0.29	0.32	0.29	0.03	4
OMe	0.12	-0.27	0.29	-0.56	1
CH_2OH	0	0	0.03	-0.03	5
OCOMe	0.39	0.31	0.42	-0.11	1
COOMe	0.37	0.45	0.34	0.11	2
NHCOMe	0.21	0	0.31	-0.31	1
CONHMe	0.35	0.36	0.35	-0.01	4
COEt	0.38	0.48	0.34	0.14	3
CH_2OCOMe	0.04	0.05	0.07	-0.02	3
$C(Me)_3$	-0.1	-0.2	-0.02	-0.18	1
C_6C1_5	0.25	0.24	0.27	-0.03	4
OC_6H_6	0.25	-0.03	0.37	-0.4	1
$(CH_2)_6CH_3$	-0.07	-0.16	0	-0.16	5
$C{=}CC_6H_6$	0.14	0.16	0.15	0.01	2

*The Hammett equation (and its extended forms) is one of the most widely used means for the study and interpretation of organic reactions and their mechanisms. Building on the success and power of the Hammett constants, efforts into further delineating the effect of field and resonance effects were undertaken. There seems to be good agreement on the magnitude of the parameter's values, hereafter called the *F* (for field) and *R* (for resonance) and generally termed Swain-Lupton values.

Table S2. Input factors and corresponding range of factors*

Factor	Range (minimum value-maximum value)
Conductivity (mS cm^{-1})	0.79 – 137.08
IEC (mmol g^{-1})	0.27 – 3.89
Water uptake (%)	5.64 – 136.1
Swelling ratio (%)	1.92 – 117
Maximum elongation (%)	1.8 – 345.45
Maximum stress /Mpa	1.8 – 310.21
Membrane thickness / um	10 – 265
Ether aryl contribution	-1.38 – 0.55
Alkyl chain contribution	-5.1 – 3.4
Sulfone contribution	-3.4 – 6.8
Spacer	-1.57 – 0.45
Extender	-2.26 – -0.39
Alkali temperature (℃)	25 – 90
Alkali concentration (mol L^{-1})	1 – 10

*All input comes from the reported literature.[6-90] In these input factors, the polymer structure information (such as alkyl chain contribution, sulfonic group contribution, ether aryl contribution, extender, spacer, and ion exchange capacity) are determined by the structure of the AEMs. The conductivity, water uptake, swelling ratio, maximum elongation, maximum stress, and membrane thickness were physical and chemical properties of AEMs. Alkali temperature and alkali concentration were operating conditions of long-term stability experiments.

Table S3. Confusion matrix describing the decision tree's predict precision on degradation rate based on the atomic numbers

	Real type	Total	Under 88% (predict)	Over 88% (predict)	Precision
Training set	Under 88%	102	102	0	100%
	Over 88%	39	1	38	97%
Testing set	Under 88%	19	12	7	60%
	Over 88%	6	3	3	50%

Table S4. Confusion matrix describing the decision tree's predict precision on degradation rate based on the Hammett substituent constants

	Real type	Total	Under 88% (predict)	Over 88% (predict)	Precision
Training set	Under 88%	102	102	0	100%
	Over 88%	39	0	39	100%
Testing set	Under 88%	19	12	7	60%
	Over 88%	6	1	5	83%

Table S5. The optimum conditions for the extraction ANN model.*

	Polymer 1	Polymer 2	Polymer 3	Polymer 4
Conductivity (30 ℃, $mS \cdot cm^{-1}$)	40.79	40.79	40.79	40.79
IEC ($mmol \cdot g^{-1}$)	1.97	1.97	1.97	1.97
Water uptake (30 ℃, %)	55.64	55.64	5.64	5.64
Swelling ratio (30 ℃, %)	1.92	2.92	2.42	3.92
Maximum elongation (%)	21.8	21.8	21.8	21.8
Maximum stress (Mpa)	9.8	9.8	61.8	61.8
Membrane thickness (um)	210	210	110	110
Ether aryl contribution	-0.11	-0.11	-0.11	-0.11
Alkyl chain contribution	-0.89	-0.89	-0.89	-0.89
Sulfone contribution	0	0	0	0
Spacer	0.39	0.39	0.28	0.28
Extender	-1.53	-1.71	-1.71	-1.53
Alkaline Temperature (℃)	60	60	60	60
Alkaline concentration ($mol \cdot L^{-1}$)	1	1	1	1
Time (h)	168	168	168	168
Predicted conductivity retention (%)	95.42	96.56	94.12	94.23

Table S5. Continued.

	Polymer 5	Polymer 6	Polymer 7	Polymer 8
Conductivity (30 ℃, $mS \cdot cm^{-1}$)	50.79	60.79	60.79	60.79
IEC ($mmol \cdot g^{-1}$)	2.27	1.27	3.27	3.27
Water uptake (30 ℃, %)	55.64	55.64	55.64	55.64
Swelling ratio (30 ℃, %)	51.92	1.92	31.92	31.92
Maximum elongation (%)	1.8	1.8	151.8	151.8
Maximum stress (Mpa)	31.8	31.8	31.8	31.8
Membrane thickness (um)	210	110	110	110
Ether aryl contribution	0	0	0	0
Alkyl chain contribution	1.0	1.0	1.0	1.0
Sulfone contribution	0	0	0	0
Spacer	0.18	0.18	0.45	0.45
Extender	-1.68	-1.83	-1.83	-1.68
Alkaline Temperature (℃)	60	60	60	60
Alkaline concentration ($mol \cdot L^{-1}$)	1	1	1	1
Time (h)	168	168	168	168
Predicted conductivity retention (%)	93.69	99.29	91.50	91.52

Table S5. Continued.

	Polymer 9	Polymer 10	Polymer 11	Polymer 12
Conductivity (30 ℃, $mS \cdot cm^{-1}$)	0.79	0.79	0.79	0.79
IEC ($mmol \cdot g^{-1}$)	0.27	0.27	0.27	0.27
Water uptake (30 ℃, %)	5.64	5.64	5.64	5.64
Swelling ratio (30 ℃, %)	1.92	1.92	1.92	1.92
Maximum elongation (%)	1.8	1.8	1.8	1.8
Maximum stress (Mpa)	1.8	1.8	1.8	1.8
Membrane thickness (um)	10	10	10	10
Ether aryl contribution	-1.38	-1.38	-1.38	-1.38
Alkyl chain contribution	-5.1	-5.1	-5.1	-5.1
Sulfone contribution	-3.4	-3.4	-0.4	-0.4
Spacer	-0.97	-0.97	-0.67	-0.67
Extender	-2.26	-1.76	-2.26	-1.76
Alkaline Temperature (℃)	60	60	60	60
Alkaline concentration ($mol \cdot L^{-1}$)	1	1	1	1
Time (h)	168	168	168	168
Predicted conductivity retention (%)	100.07	100.08	99.99	100.03

Table S5. Continued.

	Polymer 13	Polymer 14	Polymer 15	Polymer 16
Conductivity (30 ℃, mS·cm^{-1})	20.79	20.79	20.79	20.79
IEC (mmol·g^{-1})	1.27	1.27	1.27	0.27
Water uptake (30 ℃, %)	5.64	5.64	5.64	5.64
Swelling ratio (30 ℃, %)	1.92	1.92	1.92	1.92
Maximum elongation (%)	1.8	1.8	1.8	1.8
Maximum stress (Mpa)	1.8	1.8	1.8	1.8
Membrane thickness (um)	10	10	110	110
Ether aryl contribution	-1.38	-1.38	-0.18	-0.18
Alkyl chain contribution	-5.1	-5.1	2.9	2.9
Sulfone contribution	-0.4	-0.4	-3.4	-3.4
Spacer	-0.67	-0.67	-0.67	-0.67
Extender	-1.26	-0.76	-1.26	-0.76
Alkaline Temperature (℃)	60	60	60	60
Alkaline concentration (mol·L^{-1})	1	1	1	1
Time (h)	168	168	168	168
Predicted conductivity retention (%)	99.99	99.98	94.30	92.42

*For **polymers 9-12**, the conductivity of AEMs was 0.79 mS cm^{-1} and the ion exchange capacity of AEMs was 0.27. Low conductivity anion exchange membrane has no application value. Since the correspondence between polymer structure and Hammett constant is in a single direction (each substituent corresponds to a Hammett constant, while some values do not correspond to substituents), machine learning gives some

non-existent polymers. For **Polymers 13-16**, machine learning gives these prediction result: Ether aryl contribution was -1.38, Alkyl chain contribution was -5.1, and Sulfone contribution was -0.4, as far as we know, no polymer structure corresponds to these values.

Table S6. Physical and chemical properties of synthetic AEMs and operating conditions

	PPO-MTMA	PPO-ETMA	PPO-DMBA	PPO-DMHA
Conductivity ($mS \cdot cm^{-1}$)	126.68	101.82	55.99	23.16
IEC ($mmol \cdot g^{-1}$)	2.28	2.08	2.39	2.46
Water uptake (%)	47.05	39.82	50.41	103.92
Swelling ratio (%)	80.70	32.96	14.22	74.76
Membrane thickness (um)	63	48	108	97
Ether aryl contribution	-0.11	-0.11	-0.11	-0.11
Alkyl chain contribution	-0.89	-0.89	-0.89	-0.89
Sulfone contribution	0	0	0	0
Spacer	-0.17	-0.17	-0.17	-0.17
Extender	-0.51	-0.45	-0.82	-0.59
Alkaline Temperature (℃)	60	60	60	60
Alkaline concentration ($mol \cdot L^{-1}$)	1	1	1	1

Table S7. Hyperparameters of the machine learning algorithms for different purposes

Algorithm	Hyperparameter	Value/tpye
Decision tree (based on the atomic numbers)	max depth	11
	criterion	gini
Decision tree (based on the Hammett constants)	max depth	15
	criterion	gini
Gaussian Process Regressor	default	default
Supprot Vector Regressor	coef0	100
	degree	2
	epsilon	0.1
	gamma	auto
	kernel	rbf
Random Forest	max_iter	600
	max_depth	15
	max_features	auto
	min_samples_leaf	2
	min_samples_split	4

Table S7. Continued.

XGBoost	alpha	0.1
	lambda	0.1
	learning_rate	0.01
	max_depth	11
	n_estimators	8000
	objective	reg:squarederror
	subsample	0.5
Artificial Neural Network	learning_rate	0.05
	neurons	70
	Hidden layer	5
	regularizer_term	0.00001
	dropout	0
	batch_size_number	60
	activation	softsign

Reference

1 D. H. Mcdaniel, H. C. Brown, *J. Org. Chem.* **1958**, *23*, 420.

2 W. A. Sheppard, *J. Am. Chem. Soc.* **1965**, *87*, 2410.

3 H. H. Jaffe, *Chem. Rev.* **1953**, *53*, 191.

4 M. Charton, *J. Org. Chem.* **1965**, *30*, 55.

5 M. Charton, *J. Org. Chem.* **1963**, *28*, 3121.

6 X. Lin, L. Wu, Y. Liu, A. L. Ong, S. D. Poynton, J. R. Varcoe, T. Xu, *J. Power Sources* **2012**, 217, 373.

7 Y. Yang, Y. Xu, N. Ye, D. Zhang, J. Yang, R. He, *J Electrochem. Soc.* **2018**, 165, F350.

8 G. Nie, X. Li, J. Tao, W. Wu, S. Liao, *J. Membr. Sci.* **2015**, 474, 187.

9 R. A. Becerra-Arciniegas, R. Narducci, G. Ercolani, S. Antonaroli, E. Sgreccia, L. Pasquini, P. Knauth, M. L. Di Vona, *Polymer* **2019**, 185, 121931.

10 X. Qiu, M. Ueda, Y. Fang, S. Chen, Z. Hu, X. Zhang, L. Wang, *Polym. Chem.* **2016**, 7, 5988.

11 L. Liu, G. Huang, P. A. Kohl, *J. Mater. Chem. A* **2018**, 6, 9000.

12 D. W. Seo, Y. D. Lim, M. A. Hossain, S. H. Lee, H. C. Lee, H. H. Jang, S. Y. Choi, W. G. Kim, *Int. J. Hydrogen. Energ.* **2013**, 38, 579.

13 M. M. Hossain, L. Wu, X. Liang, Z. Yang, J. Hou, T. Xu, *J. Power Sources* **2018**, 390, 234.

14 N. A. Qaisrani, L. Ma, J. Liu, M. Hussain, L. Li, P. Li, S. Gong, F. Zhang, G. He, *J. Membr. Sci.* **2019**, 581, 293.

15 Z. Zhang, K. Shen, L. Lin, J. Pang, *J. Membr. Sci.* **2016**, 497, 318.

16 X. Q. Wang, C. X. Lin, Q. G. Zhang, A. M. Zhu, Q. L. Liu, *Int. J. Hydrogen. Energ.* **2017**, 42, 19044.

17 C. Wang, Z. Tao, Y. Zhou, X. Zhao, J. Li, Q. Ren, M. D. Guiver, *Sci. China Mater.* **2020**, 63, 2539.

18 F. H. Liu, C. X. Lin, E. N. Hu, Q. Yang, Q. G. Zhang, A. M. Zhu, Q. L. Liu, *J. Membr. Sci.* **2018**, 564, 298.

19 C. M. Tuan, D. Kim, *J. Membr. Sci.* **2016**, 511, 143.

20 A. N. Lai, L. S. Wang, C. X. Lin, Y. Z. Zhuo, Q. G. Zhang, A. M. Zhu, Q. L. Liu, *J. Membr. Sci.* **2015**, 481, 9.

21 X. Zhang, P. Chen, Q. Shi, S. Li, F. Gong, X. Chen, Z. An, *Int. J. Hydrogen Energ.* **2017**, 42, 26320.

22 X. Zhang, Q. Shi, P. Chen, J. Zhou, S. Li, H. Xu, X. Chen, Z. An, *Polymer Chem.* **2018**, 9, 699.

23 A. Amel, N. Yitzhack, A. Beylin, J. Pan, M. A. Hickner, Y. Ein-Eli, *J. Electrochem. Soc.***2018**, 165, F1133.

24 Q. Ge, J. Ran, J. Miao, Z. Yang, T. Xu, *ACS Appl. Mater. Interfaces* **2015**, 7, 28545.

25 M. Zhu, X. Zhang, Y. Su, Y. Wang, Y. Wu, D. Yang, H. Wang, M. Zhang, M. Zhang, Q. Chen, N. Li, *J. Appl. Polymer Sci.* **2019**, 136, 47370.

26 A. N. Lai, Z. Wang, Q. Yin, R. Y. Zhu, P. C. Hu, J. W. Zheng, S. F. Zhou, *Int. J. Hydrogen Energ.* **2020**, 45, 11148.

27 D. Yao, T. Wei, L. Shang, H. Na, C. Zhao, *RSC Advances* **2019**, 9, 7975.

28 K. Firouz Tadavani, A. Abdolmaleki, M. R. Molavian, M. Zhiani, *Energ. Fuels* **2019**, 33, 12016.

29 B. Wang, W. Sun, F. Bu, X. Li, H. Na, C. Zhao, *Int. J. Hydrogen Energ.* **2016**, 41, 3102.

30 L. An, T. S. Zhao, Q. X. Wu, L. Zeng, *Int. J. Hydrogen Energ.* **2012**, 37, 14536.

31 S. Zhang, X. Zhu, C. Jin, *J. Mater. Chem. A* **2019**, 7, 6883.

32 A. Carbone, R. Pedicini, I. Gatto, A. Sacca, A. Patti, G. Bella, M. Cordaro, *Polymers* **2020**, 12

33 J. Ran, C. Fu, L. Ding, P. Cao, T. Xu, *J. Mater. Chem. A* **2018**, 6, 5714.

34 S. Sung, M. T.S, J. E. Chae, H.-J. Kim, T.-H. Kim, *J. Indust.Engineer. Chem.* **2020**, 81, 124.

35 L. Zeng, T. S. Zhao, *J. Power Sources* **2016**, 303, 354.

36 S.-B. Lee, C.-M. Min, J. Jang, J.-S. Lee, *Polymer* **2020**, 192, 122331.

37 Z. Li, X. He, Z. Jiang, Y. Yin, B. Zhang, G. He, Z. Tong, H. Wu, K. Jiao, *Electrochim Acta* **2017**, 240, 486.

38 F. Xie, Z. Shao, X. Gao, J. Hao, W. Song, H. Yu, B. Yi, *Solid State Ionics* **2019**, 338, 58.

39 M. Zhang, C. Shan, L. Liu, J. Liao, Q. Chen, M. Zhu, Y. Wang, L. An, N. Li, *ACS Appl. Mater. Interfaces* **2016**, 8, 23321.

40 P. Yu Xu, K. Zhou, G. Lu Han, Q. Gen Zhang, A. Mei Zhu, Q. Lin Liu, *J. Membr. Sci.* **2014**, 457, 29.

41 J. Chen, C. Li, J. Wang, L. Li, Z. Wei, *J. Mater. Chem. A* **2017**, 5, 6318.

42 H. Zarrin, J. Wu, M. Fowler, Z. Chen, *J. Membr. Sci.* **2012**, 394-395, 193.

43 J. Ponce-González, D. K. Whelligan, L. Wang, R. Bance-Soualhi, Y. Wang, Y. Peng, H. Peng, D. C. Apperley, H. N. Sarode, T. P. Pandey, A. G. Divekar, S. Seifert, A. M. Herring, L. Zhuang, J. R. Varcoe, *Energ. Environ. Sci.* **2016**, 9, 3724.

44 J. Ran, L. Wu, Q. Ge, Y. Chen, T. Xu, *J. Membr. Sci.* **2014**, 470, 229.

45 C. Qu, H. Zhang, F. Zhang, B. Liu, *J. Mater. Chem.* **2012**, 22, 8203.

46 S. Li, J. Pang, Z. Chen, D. Liu, Y. Han, K. Wang, S. Huang, Z. Jiang, *J. Membr. Sci.* **2019**, 589.

47 C. Yang, L. Liu, X. Han, Z. Huang, J. Dong, N. Li, *J. Mater. Chem. A* **2017**, 5, 10301.

48 J. Ran, L. Ding, C. Chu, X. Liang, T. Pan, D. Yu, T. Xu, *J. Mater. Chem. A* **2018**, 6, 17101.

49 C. Jin, X. Zhu, S. Zhang, *Solid State Ionics* **2019**, 335, 121.

50 N. Li, Y. Leng, M. A. Hickner, C. Y. Wang, *J. Am. Chem. Soc.* **2013**, 135, 10124.

51 H. Lim, T. H. Kim, *Macromol. Res.* **2017**, 25, 1220.

52 C. Lin, X. Liu, Q. Yang, H. Wu, F. Liu, Q. Zhang, A. Zhu, Q. Liu, *J. Membr. Sci.* **2019**, 585, 90.

53 A. Z. Al Munsur, I. Hossain, S. Y. Nam, J. E. Chae, T.-H. Kim, *J. Membr. Sci.* **2020**, 599, 117829.

54 R. He, P. Wen, H.-N. Zhang, S. Guan, G. Xie, L.-Z. Li, M.-H. Lee, X.-D. Li, *J. Membr. Sci.* **2018**, 556, 73.

55 Y. He, L. Wu, J. Pan, Y. Zhu, X. Ge, Z. Yang, J. Ran, T. Xu, *J. Membr. Sci.* **2016**, 504, 47.

56 L. Li, X. Yue, W. Wu, W. Yan, M. Zeng, Y. Zhou, S. Liao, X. Li, *RSC Advances* **2016**, 6, 41453.

57 X. Dong, B. X. Xue, H. D. Qian, J. F. Zheng, S. H. Li, S. B. Zhang, *J. Power Sources* **2017**, 342, 605.

58 D. Koronka, A. Matsumoto, K. Otsuji, K. Miyatake, *Rsc Advances* **2019**, 9, 37391.

59 X. Li, K. Wang, D. Liu, L. Lin, J. Pang, *Polymer* **2020**, 195, 122456.

60 E. N. Hu, C. X. Lin, F. H. Liu, X. Q. Wang, Q. G. Zhang, A. M. Zhu, Q. L. Liu, *J. Membr. Sci.* **2018**, 550, 254.

61 Q. Shi, P. Chen, J. Zhou, Q. Weng, X. Zhang, X. Chen, Z. An, *RSC Advances* **2017**, 7, 30770.

62 M. S. Cha, J. E. Park, S. Kim, S.-H. Han, S.-H. Shin, S. H. Yang, T.-H. Kim, D. M. Yu, S. So, Y. T. Hong, S. J. Yoon, S.-G. Oh, S. Y. Kang, O.-H. Kim, H. S. Park, B. Bae, Y.-E. Sung, Y.-H. Cho, J. Y. Lee, *Energ. Environ. Sci.* **2020**, 13, 3633.

63 W. Mei, Z. Wang, J. Yan, *Polymer* **2017**, 125, 265.

64 B. Shen, H. Pu, *Polymer* **2020**, 207, 122944.

65 T. S. Mayadevi, S. Sung, L. Varghese, T. H. Kim, *Membranes* **2020**, 10, 329.

66 H.-S. Dang, E. A. Weiber, P. Jannasch, *J. Mater. Chem. A* **2015**, 3, 5280.

67 V. Yadav, A. Rajput, P. P. Sharma, P. K. Jha, V. Kulshrestha, *Coll. Surf. A: Physic. Engin. Aspects* **2020**, 588, 124348.

68 X. Wang, W. Chen, X. Yan, T. Li, X. Wu, Y. Zhang, F. Zhang, B. Pang, G. He, *J. Power Sources* **2020**, 451, 227813.

69 M. Irfan, E. Bakangura, N. U. Afsar, M. M. Hossain, J. Ran, T. Xu, *J. Power Sources* **2017**, 355, 171.

70 K. Yang, X. Li, J. Guo, J. Zheng, S. Li, S. Zhang, X. Cao, T. A. Sherazi, X. Liu, *J. Membr. Sci.* **2020**, 596, 117720.

71 S. Lee, H. Lee, T. H. Yang, B. Bae, N. A. T. Tran, Y. Cho, N. Jung, D. Shin, *Membranes* **2020**, 10, 306.

72 T. S. Mayadevi, S. Sung, J. E. Chae, H.-J. Kim, T.-H. Kim, *Int. J. Hydrogen Energ.* **2019**, 44, 18403.

73 W. Sheng, X. Zhou, L. Wu, Y. Shen, Y. Huang, L. Liu, S. Dai, N. Li, *J. Membr. Sci.* **2020**, 601, 117881.

74 C. Xiao Lin, X. Qin Wang, E. Ning Hu, Q. Yang, Q. Gen Zhang, A. Mei Zhu, Q. Lin Liu, *J. Membr. Sci.* **2017**, 541, 358.

75 J. Hou, Y. Liu, Q. Ge, Z. Yang, L. Wu, T. Xu, *J. Power Sources* **2018**, 375, 404.

76 C. X. Lin, X. L. Huang, D. Guo, Q. G. Zhang, A. M. Zhu, M. L. Ye, Q. L. Liu, *J. Mater. Chem. A* **2016**, 4, 13938.

77 Y. L. Jiang, J. B. Liao, S. S. Yang, J. Li, Y. Q. Xu, H. M. Ruan, A. Sotto, B. Van der Bruggen, J. N. Shen, *React Funct Polym* **2018**, 130, 61.

78 J. Y. Chu, K. H. Lee, A. R. Kim, D. J. Yoo, *Acs Sustain Chem Eng* **2019**, 7, 20077.

79 E. Kim, S. Lee, S. Woo, S.-H. Park, S.-D. Yim, D. Shin, B. Bae, *J. Power Sources* **2017**, 359, 568.

80 J. Pan, Z. Sun, H. Zhu, H. Cao, B. Wang, J. Zhao, F. Yan, *J. Membr. Sci.* **2020**, 610, 118283.

81 K. Shen, J. Pang, S. Feng, Y. Wang, Z. Jiang, *J. Membr. Sci.* **2013**, 440, 20.

82 Q. Shi, P. Chen, X. Zhang, Q. Weng, X. Chen, Z. An, *Polymer* **2017**, 121, 137.

82 M. Zhu, Y. Su, Y. Wu, M. Zhang, Y. Wang, Q. Chen, N. Li, *J. Membr. Sci.* **2017**, 541, 244.

83 W. Wu, B. Wei, J. Feng, B. Chi, S. Liao, X. Li, Y. Yu, *Macromolecular Chem. Phy.* **2018**, 219, 17000416.

84 F. Wang, B. Xue, S. Zhou, J. Zheng, S. Li, S. Zhang, T. A. Sherazi, *J. Membr. Sci.* **2019**, 591, 117334.

85 M. Zhu, M. Zhang, Q. Chen, Y. Su, Z. Zhang, L. Liu, Y. Wang, L. An, N. Li, *Polym. Chem.* **2017**, 8, 2074.

86 X. Du, H. Zhang, Y. Yuan, Z. Wang, J. Xu, *Int. J. Hydrogen Energ.* **2020**, 45, 11814.

87 Y. Zhang, W. Chen, T. Li, X. Yan, F. Zhang, X. Wang, X. Wu, B. Pang, G. He, *J. Membr. Sci.* **2020**, 613.

88 S. Huang, X. He, Y. Guo, D. Chen, *Polymer* **2020**, 206, 122883.

89 L. Liu, X. Chu, J. Liao, Y. Huang, Y. Li, Z. Ge, M. A. Hickner, N. Li, *Energ. Environ. Sci.* **2018**, 11, 435.

90 G. Shukla, V. K. Shahi, *Int. J. Hydrogen Energ.* **2018**, 43, 21742.